Aalto University

OPEN ACCESS

This is an electronic reprint of the original article.
This reprint may differ from the original in pagination and typographic detail.

Korhonen, Esa; Tuomisto, F.; Gogova, D.; Wagner, G.; Baldini, M.; Galazka, Z.; Schewski, R.; Albrecht, M.

# Electrical compensation by Ga vacancies in $Ga_2O_3$ thin films

*Published in:*
Applied Physics Letters

*DOI:*
10.1063/1.4922814

Published: 01/01/2015

*Document Version*
Publisher's PDF, also known as Version of record

*Please cite the original version:*
Korhonen, E., Tuomisto, F., Gogova, D., Wagner, G., Baldini, M., Galazka, Z., Schewski, R., & Albrecht, M. (2015). Electrical compensation by Ga vacancies in $Ga_2O_3$ thin films. *Applied Physics Letters*, *106*(24), 1-3. Article 242103. https://doi.org/10.1063/1.4922814

This material is protected by copyright and other intellectual property rights, and duplication or sale of all or part of any of the repository collections is not permitted, except that material may be duplicated by you for your research use or educational purposes in electronic or print form. You must obtain permission for any other use. Electronic or print copies may not be offered, whether for sale or otherwise to anyone who is not an authorised user.

.

# Electrical compensation by Ga vacancies in $Ga_2O_3$ thin films

E. Korhonen, F. Tuomisto, D. Gogova, G. Wagner, M. Baldini, Z. Galazka, R. Schewski, and M. Albrecht

Citation: Appl. Phys. Lett. **106**, 242103 (2015); doi: 10.1063/1.4922814
View online: http://dx.doi.org/10.1063/1.4922814
View Table of Contents: http://aip.scitation.org/toc/apl/106/24
Published by the American Institute of Physics

**Articles you may be interested in**

Oxygen vacancies and donor impurities in $\beta-Ga_2O_3$
Applied Physics Letters **97**, 142106 (2010); 10.1063/1.3499306

Gallium oxide ($Ga_2O_3$) metal-semiconductor field-effect transistors on single-crystal $\beta$-$Ga_2O_3$ (010) substrates
Applied Physics Letters **100**, 013504 (2012); 10.1063/1.3674287

Crystal Structure of $\beta$-$Ga_2O_3$
The Journal of Chemical Physics **33**, 676 (2004); 10.1063/1.1731237

Electrical properties of $\beta$-$Ga_2O_3$ single crystals grown by the Czochralski method
Journal of Applied Physics **110**, 063720 (2011); 10.1063/1.3642962

Intrinsic electron mobility limits in $\beta$-$Ga_2O_3$
Applied Physics Letters **109**, 212101 (2016); 10.1063/1.4968550

Deep level defects throughout the bandgap of (010) $\beta$-$Ga_2O_3$ detected by optically and thermally stimulated defect spectroscopy
Applied Physics Letters **108**, 052105 (2016); 10.1063/1.4941429

# Electrical compensation by Ga vacancies in $Ga_2O_3$ thin films

E. Korhonen,[1] F. Tuomisto,[1] D. Gogova,[2] G. Wagner,[2] M. Baldini,[2] Z. Galazka,[2] R. Schewski,[2] and M. Albrecht[2]
[1]*Department of Applied Physics, Aalto University, 00076 Aalto, Finland*
[2]*Leibniz Institute for Crystal Growth, 12489 Berlin, Germany*

(Received 10 April 2015; accepted 8 June 2015; published online 17 June 2015)

The authors have applied positron annihilation spectroscopy to study the vacancy defects in undoped and Si-doped $Ga_2O_3$ thin films. The results show that Ga vacancies are formed efficiently during metal-organic vapor phase epitaxy growth of $Ga_2O_3$ thin films. Their concentrations are high enough to fully account for the electrical compensation of Si doping. This is in clear contrast to another *n*-type transparent semiconducting oxide $In_2O_3$, where recent results show that *n*-type conductivity is not limited by cation vacancies but by other intrinsic defects such as $O_i$. © *2015 AIP Publishing LLC*. [http://dx.doi.org/10.1063/1.4922814]

Transparent semiconducting oxides (TSOs), such as $In_2O_3$, $SnO_2$, ZnO, and $Ga_2O_3$, combine electrical conductivity with optical transparency which makes them an important material category for electronics and optoelectronics. In highly doped and conducting form (transparent conducting oxides, TCOs), they have applications as transparent contacts in the fields of photovoltaic devices, liquid crystal displays, and light emitting diodes.

$Ga_2O_3$ has recently generated significant interest and high quality growth (both thin-film and bulk) has been achieved with several techniques.[1–7] Its distinctive feature compared to other TSOs is the high transparency all the way to UV due to a wide optical 4.9 eV band gap, thus it is a possible material for future UV devices. $Ga_2O_3$ may crystallize in several different lattice configurations, of which the monoclinic $\beta$-$Ga_2O_3$ is the most commonly considered due to its stability. In a perfect stoichiometric form $Ga_2O_3$ is an insulator. Extrinsic *n*-doping has been achieved with Sn, while undoped $Ga_2O_3$ thin films are *n*-type conductive when grown under low $O_2$ partial pressure.[8] Oxygen vacancies have been suggested as the origin of intrinsic *n*-type conductivity,[9] but recent theoretical calculations find $V_O$ to be a deep donor,[10] leaving this question open. Si has been predicted to be an efficient *n*-dopant[10] and Si-doping has been successfully demonstrated with $Ga_2O_3$ bulk crystals.[11,12] *p*-doping seems to still elude researchers, similarly to many other TSOs.

In order to use $Ga_2O_3$ as a semiconductor in electronics, detailed understanding and control of defects and doping are required. Positron annihilation spectroscopy is a powerful method for studying vacancy defects in semiconductors.[13] In this work, we use positrons to investigate vacancy type defects in undoped and Si-doped $Ga_2O_3$. We find that the concentrations of Ga vacancy related defects are high enough to fully explain the electrical compensation.

A series of thin-film $Ga_2O_3$ samples were prepared using Metal-Organic Vapor Phase Epitaxy (MOVPE) in low pressure mode on both *n*-type conductive $Ga_2O_3$ (series G) substrates cut from Czochralski-grown bulk single crystals,[3,14] and insulating $Al_2O_3$ (series A). All samples were grown at oxygen-rich conditions at 800 °C, with trimethylgallium as Ga source, $H_2O$ as oxygen source, and tetraethylorthosilicate as Si source. Growth on $Al_2O_3$ (0001) resulted in polycrystalline, yet epitaxial (relationship with the substrate but with in-plane tilt) growth.[15] Homoepitaxial growth resulted in single crystalline material.[16] Growth parameters, most notably Si concentration, were varied for different samples. Basic sample information can be found in Table I. The dopant concentration was measured using secondary ion mass spectrometry employing a Si implanted bulk $\beta$-$Ga_2O_3$ standard. Electrical properties were measured by Hall effect measurements. All thin-film samples were found to be electrically insulating, even the ones with heaviest Si doping.

Positron annihilation spectroscopy is based on implanting the target with positrons and detecting the 511 keV gamma quanta produced by the subsequent electron-positron annihilation. Since positrons are repelled by the positive charge of the atom cores, neutral and negatively charged vacancy defects often act as positron traps. In a vacancy, both the electron density and average electron momentum are reduced compared to the lattice. A positron localized at a vacancy has an increased lifetime as well as an increased probability to annihilate with a low momentum valence electron compared to a delocalized positron. The change in the electron momentum distribution can be seen in the Doppler shift of the annihilation gamma spectrum. To describe the spectrum in a brief fashion, two parameters $S$ and $W$ are typically used.[13] $S$ is the relative number of counts in the central area of the peak and its value is usually close to 0.5. $W$ is the relative number of counts in the high momentum areas on both sides of the peak. Typically, an increase in the value of $S$ indicates an increase in open volume defects in the depth being probed, mainly due to the reduced overlap of the positron wavefunction with core electron wavefunctions when the positron is trapped in a vacancy. The value of $W$ is more dependent on the type of atoms surrounding the annihilation site.

A variable-energy slow positron beam was used to measure the thin-film samples. The kinetic energy of the positrons was varied to probe varying depths in the samples. The results are shown in Figures 1 and 2 which show the $S$ parameter as a function of implantation energy for most of the samples. The corresponding mean implantation depth is marked on the top axis.

Starting from the low energies, the values of the first two data points in the plots are heavily affected by the

 © 2015 AIP Publishing LLC

TABLE I. Sample thicknesses and dopant concentrations. The MOVPE reactor pressure was 5 mbar for all samples except A5, G1, and G2. Label A stands for $Al_2O_3$ and G for $Ga_2O_3$ substrate.

| Sample number | d (nm) | [Si] ($cm^{-3}$) | Notes |
|---|---|---|---|
| A1 | 262 | $1.0 \times 10^{16}$ | … |
| A2 | 260 | $2.2 \times 10^{16}$ | … |
| A3 | 251 | $1.1 \times 10^{17}$ | … |
| A4 | 261 | $2.5 \times 10^{17}$ | … |
| A5 | 256 | $3.5 \times 10^{17}$ | $P_{base} = 10$ mbar |
| A6 | 290 | $\approx 10^{17}$–$10^{18}$ $cm^{-3}$ | … |
| G1 | 200 | … | $P_{base} = 10$ mbar |
| G2 | 200 | … | Ann. in 1 atm $O_2$ at 950 °C, $P_{base} = 10$ mbar |
| G3 | 200 | … | Ann. in 1 atm $O_2$ at 950 °C |
| G4 | 290 | $\approx 10^{17}$–$10^{18}$ $cm^{-3}$ | … |

surface due to diffusion of thermalized positrons. At 3 keV most of the *S*-parameters reach their minimum values within the layer area and the surface contribution to the signal is low.

Between 3 and 6 keV the *S*-value increases slightly to a maximum value in several samples of the A-series. At 6 keV, the mean implantation depth (and the distribution width) is 120 nm. Consequently, a significant fraction of positrons reaches the region at the $Ga_2O_3/Al_2O_3$ heterointerface. This region is likely to contain a higher amount of defects compared to the layer, which is seen as a higher value of *S*. Other samples lack this effect; G1 and G2 do not even show any plateau in the *S*-value. The lack of a distinguishable interface state can be attributed to homoepitaxial growth.

The stationary positron diffusion equation was fitted with VEPFIT[17] to the (S, E) and (W, E) data of samples G1 and G2 in order to extract the layer-specific parameters. A simple model with one layer on top of a substrate was applied. The fitting gave effective positron diffusion lengths of about 10 nm in the $Ga_2O_3$ thin films and about 100 nm in the substrate. G3 and G4 did not require fitting, as the layer-specific value could be read directly from the data.

Above 6 keV, a higher and higher fraction of positrons is implanted to the substrate. All of the data points eventually converge to either the $Al_2O_3$ or the $Ga_2O_3$ substrate value, 0.431 or 0.445, respectively.

For detailed analysis of the positron data, a data point (*S*, *W*-value pair) for a low defect density ($<10^{16}$ $cm^{-3}$ vacancies) crystal is very useful as a reference. A positron lifetime measurement[13] is of particular use for determining this property and it requires a bulk crystal sample. Samples G1 and G4 served as the sample pair for the lifetime measurement with their $Ga_2O_3$ substrates. The result of the lifetime measurement was a single lifetime of 176 ps with a 260 ps FWHM spectrometer. A similar value has been reported earlier for a free positron in $Ga_2O_3$.[18] Hence, it is likely that the $Ga_2O_3$ substrate produces *S* and *W* parameters representative of the $Ga_2O_3$ lattice and that these can be used as reference values. They are obtained by averaging the *S* and *W* data from the energy range (15–23 keV) in the sample G1, giving $S = 0.445$ and $W = 0.0497$. The long positron diffusion length of the substrate obtained above also supports this conclusion.

In order to analyze in detail the differences in annihilation parameters in the $Ga_2O_3$ layers between different samples, an *S*–*W*-plot is shown in Fig. 3. One point was drawn for each sample. These layer (*S*, *W*)-value pairs are determined either by taking the corresponding average from the energy range of 2–6 keV, although the exact range was varied from sample to sample to take into account the different layer thicknesses, or from fitting the stationary positron diffusion equation. The error bars indicate the statistical uncertainty within the selected energy range. Thus, these values best represent the positron state in the thin-layer. In Fig. 3, the points lie on a line with the bulk point on the one end and with samples A1 to A4 on the other. The bulk point has the

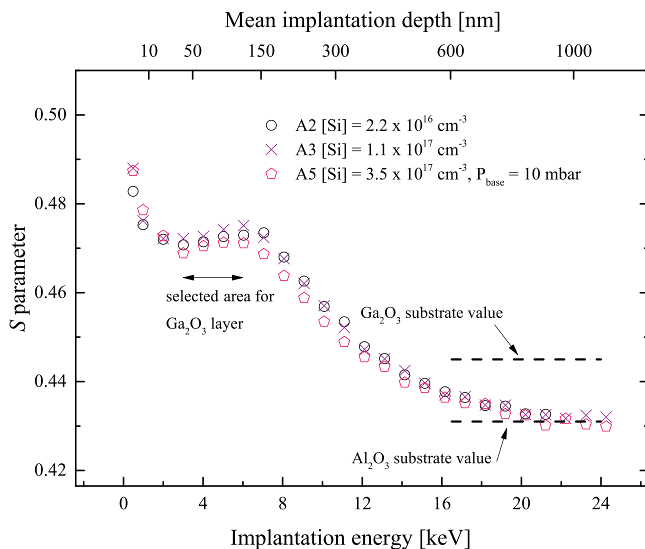


FIG. 1. *S* parameter as a function of implantation energy for a selection of samples grown on $Al_2O_3$. The substrate and layer areas are clearly distinguishable. The range marked as "selected area" is used for calculating the layer values for Fig. 3.

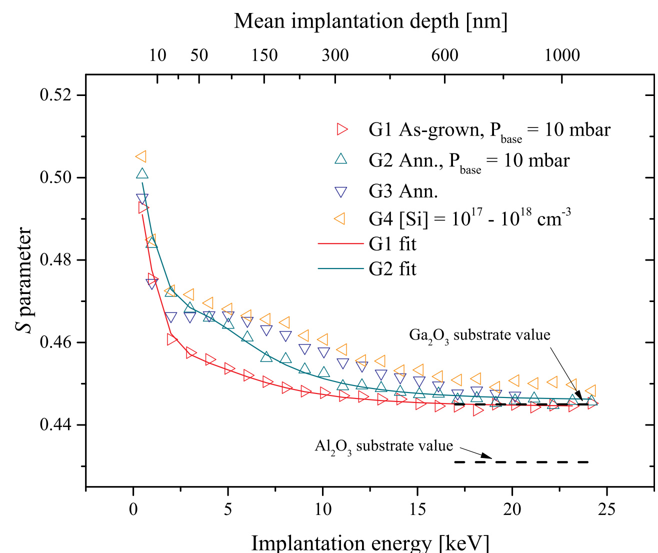


FIG. 2. *S* parameter as a function of implantation energy for samples grown on $Ga_2O_3$. The solid curves are obtained by fitting the stationary positron diffusion equation to the data.

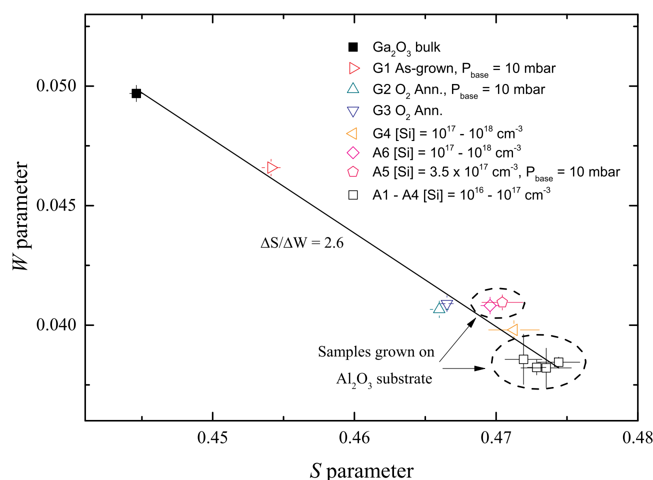


FIG. 3. $S-W$-plot with all samples included. One point is drawn per sample for easy comparison. A linear best fit to the points is shown.

lowest $S$ and highest $W$-values due to positrons annihilating mostly in the free state in the bulk.

A linear change in ($S$, $W$) is usually the case when positron trapping is dominated by one defect type. The vacancy in question must be Ga-related since single oxygen vacancies are too small to trap positrons in addition to usually being positively charged.[19] The simplest explanation is that single gallium vacancies ($V_{Ga}$) are detected, although complexes of $V_{Ga}$ with $V_O$ are possible as well.

Several of the samples in the heteroepitaxial A series (A1–A4) form a tight cluster near the low right corner with $S = 0.471$–$0.475$ and $W = 0.038$. Changing the Si-doping concentration has very little effect on the positron results as long as other growth parameters are kept constant. It is likely that the cluster of points represents the vacancy state with all positrons being trapped to vacancies in the corresponding samples. Comparing the $S$ and $W$-values of this state $(S_D, W_D) = [0.474(2), 0.038(1)]$ with those of the bulk state $(S_B, W_B) = [0.445(1), 0.050(1)]$ gives the characteristic value $S_D/S_B = 1.066(6)$ and $W_D/W_B = 0.76(2)$. Similar values (1.058 and 0.76) have been measured for $V_{Ga}$ in GaN,[20] a material with constituent atom sizes close to those of $Ga_2O_3$. In addition, the vacancy signal gets stronger with annealing in $O_2$, supporting this interpretation. Saturation trapping implies that the $V_{Ga}$ concentration in the samples A1–A4 is at least $5 \times 10^{18}\,cm^{-3}$.[13]

Samples of the homoepitaxial G-series, as well as A5 and A6, fall between the line endpoints. The layer of sample G1 is clearly closest to the bulk point. This sample was not treated in any way after growth. The annealed samples G2 and G3 are significantly further away and give practically identical results. A5 and A6 have similar growth parameters but were grown in different batches. Finally, G4 is a homoepitaxial version of A6 and is located a bit further down the line. The vacancy concentration of these samples can be estimated by comparing the annihilation parameters to those of the defect and the defect-free lattice as in Ref. 21. In G1, the concentration is $1 \times 10^{17}\,cm^{-3}$, in G2 and G3 $5 \times 10^{17}\,cm^{-3}$, and finally in A5, A6, and G4 in the $1$–$2 \times 10^{18}\,cm^{-3}$ range. Both annealing in $O_2$ and Si doping strongly increase the concentration of Ga vacancies in the samples.

All thin-film samples were found to be electrically insulating despite significant Si-doping. The Ga vacancy concentration is highest in the samples A1–A4 that were Si-doped from $10^{16}$ to $10^{17}\,cm^{-3}$. This is less than the estimated Ga vacancy concentration ($>5 \times 10^{18}\,cm^{-3}$). Theoretical calculations predict that the $V_{Ga}$ should be in a negative charge state for Fermi levels in the upper half of the band gap,[22] compensating for $n$-type doping. Hence, the observed Ga vacancy concentrations in the $Ga_2O_3$ films fully account for the compensation of Si doping. In addition, the $n$-type conductive substrate does not contain a significant concentration of Ga vacancies, in line with this conclusion.

In summary, homo- and heteroepitaxial undoped and Si-doped $Ga_2O_3$ thin films were studied using positron annihilation spectroscopy. All samples show a significant (above $10^{17}\,cm^{-3}$) concentration of Ga vacancies, enough to fully explain the electrical compensation. Interestingly, this finding is opposite to that in $In_2O_3$,[21] where $n$-type conductivity is not limited by cation vacancies but by other intrinsic defects such as $O_i$.

This work was supported by the Academy of Finland.

[1]E. G. Víllora, K. Shimamura, Y. Yoshikawa, K. Aoki, and N. Ichinose, J. Cryst. Growth **270**, 420 (2004).
[2]H. Aida, K. Nishiguchi, H. Takeda, N. Aota, K. Sunakawa, and Y. Yaguchi, Jpn. J. Appl. Phys. **47**, 8506 (2008).
[3]Z. Galazka, K. Irmscher, R. Uecker, R. Bertram, M. Pietsch, A. Kwasniewski, M. Naumann, T. Schulz, R. Schewski, D. Klimm, and M. Bickermann, J. Cryst. Growth **404**, 184 (2014).
[4]H. Murakami, K. Nomura, K. Goto, K. Sasaki, K. Kawara, Q. T. Thieu, R. Togashi, Y. Kumagai, M. Higashiwaki, A. Kuramata *et al.*, Appl. Phys. Express **8**, 015503 (2015).
[5]M. Orita, H. Ohta, M. Hirano, and H. Hosono, Appl. Phys. Lett. **77**, 4166 (2000).
[6]K. Sasaki, A. Kuramata, T. Masui, E. G. Víllora, K. Shimamura, and S. Yamakoshi, Appl. Phys. Express **5**, 035502 (2012).
[7]X. Du, W. Mi, C. Luan, Z. Li, C. Xia, and J. Ma, J. Cryst. Growth **404**, 75 (2014).
[8]N. Ueda, H. Hosono, R. Waseda, and H. Kawazoe, Appl. Phys. Lett. **70**, 3561 (1997).
[9]Z. Hajnal, J. Miró, G. Kiss, F. Réti, P. Deák, R. C. Herndon, and J. M. Kuperberg, J. Appl. Phys. **86**, 3792 (1999).
[10]J. Varley, J. Weber, A. Janotti, and C. Van de Walle, Appl. Phys. Lett. **97**, 142106 (2010).
[11]E. G. Víllora, K. Shimamura, Y. Yoshikawa, T. Ujiie, and K. Aoki, Appl. Phys. Lett. **92**, 202120 (2008).
[12]K. Sasaki, M. Higashiwaki, A. Kuramata, T. Masui, and S. Yamakoshi, Appl. Phys. Express **6**, 086502 (2013).
[13]F. Tuomisto and I. Makkonen, Rev. Mod. Phys. **85**, 1583 (2013).
[14]Z. Galazka, R. Uecker, K. Irmscher, M. Albrecht, D. Klimm, M. Pietsch, M. Brützam, R. Bertram, S. Ganschow, and R. Fornari, Cryst. Res. Technol. **45**, 1229 (2010).
[15]D. Gogova, G. Wagner, M. Baldini, M. Schmidbauer, K. Irmscher, R. Schewski, Z. Galazka, M. Albrecht, and R. Fornari, J. Cryst. Growth **401**, 665 (2014).
[16]G. Wagner, M. Baldini, D. Gogova, M. Schmidbauer, R. Schewski, M. Albrecht, Z. Galazka, D. Klimm, and R. Fornari, Phys. Status Solidi A **211**, 27 (2014).
[17]A. Van Veen, H. Schut, J. De Vries, R. Hakvoort, and M. Ijpma, AIP Conf. Proc. **218**, 171–198 (1991).
[18]W.-Y. Ting, A. H. Kitai, and P. Mascher, Mater. Sci. Eng., B **91**, 541 (2002).
[19]C. Rauch, I. Makkonen, and F. Tuomisto, Phys. Rev. B **84**, 125201 (2011).
[20]F. Tuomisto, A. Pelli, K. Yu, W. Walukiewicz, and W. Schaff, Phys. Rev. B **75**, 193201 (2007).
[21]E. Korhonen, F. Tuomisto, O. Bierwagen, J. S. Speck, and Z. Galazka, Phys. Rev. B **90**, 245307 (2014).
[22]J. Varley, H. Peelaers, A. Janotti, and C. Van de Walle, J. Phys.: Condens. Matter **23**, 334212 (2011).